Title
Self-assembly for electronics

Journal
MRS Bulletin, 45(10)

ISSN
0883-7694

Authors
Kagan, Cherie R
Hyeon, Taeghwan
Kim, Dae-Hyeong
et al.

Publication Date
2020-10-01

DOI
10.1557/mrs.2020.248

Peer reviewed

Self-assembly for electronics

Cherie R Kagan, Taeghwan Hyeon, Dae-Hyeong Kim,
Ricardo Ruiz,* Maryann C. Tung,and H.S. Philip Wong

Self-assembly, a process in which molecules, polymers, and particles are driven by local interactions to organize into patterns and functional structures, is being exploited in advancing silicon electronics and in emerging, unconventional electronics. Silicon electronics has relied on lithographic patterning of polymer resists at progressively smaller lengths to scale down device dimensions. Yet, this has become increasingly diffi cult and costly. Assembly of block copolymers and colloidal nanoparticles allows resolution enhancement and the defi nition of essential shapes to pattern circuits and memory devices. As we look to a future in which electronics are integrated at large numbers and in new forms for the Internet of Things and wearable and implantable technologies, we also explore a broader material set. Semiconductor nanoparticles and biomolecules are prized for their size-, shape-, and composition-dependent properties and for their solution-based assembly and integration into devices that is enabling unconventional manufacturing and new device functions.

Introduction

Electronics are pervasive as sensing, communication, and computation devices, with continued growth in demand for "conventional" consumer electronic goods (e.g., cameras, computers, and tablets) and "unconventional" applications to support the Internet of Things, mobile, wearable, and implantable technologies. Conventional and unconventional electronics often require patterning to scale down device size and enhance performance; on the other hand, processing over large areas and the introduction and integration of a broader range of materials are also required to realize both function and form. Fabrication techniques are typically "top-down" processes in the electronics industry. However, the demands for small-scale, large-area, more functional, and flexible forms for devices are motivating research and commercial adoption of "bottom-up" synthesis and assembly methods for materials and devices.

Here, we describe through examples, the self- and directed self-assembly of molecules, polymers, and nanoparticles (NPs) being exploited for their structure and function to advance electronic devices.

Block copolymers and their assembly

Self-assembly of block copolymers (BCPs) has been extensively researched for lithographic applications due to its ability to form uniform features at the nanometer scale. BCPs consist of chemically distinct, covalently bonded homopolymers. Provided sufficient thermal energy, free-energy minimization drives BCPs to self-assemble into a myriad of morphologies depending on the relative volume fractions of the constituent homopolymers.[1] Of particular interest to chipmakers are lamellar and cylindrical phase diblock copolymers that can be used to pattern lines and holes, respectively. The size and pitch of the self-assembled lamellae and cylinders can be set by varying the polymer length, allowing BCP lithography to reach sub-10 nm resolutions.[2] Integration with lithography additionally provides guiding features for directed self-assembly (DSA) to achieve domain registration and placement control.

For semiconductor technology

Directed self-assembly was initially envisioned as a method to extend the resolution of 193-nm immersion (193i) lithography.

Cherie R Kagan, University of Pennsylvania, USA; kagan@seas.upenn.edu
Taeghwan Hyeon, Center for Nanoparticle Research of the Institute for Basic Science, and School of Chemical and Biological Engineering, Seoul National University, South Korea; thyeon@snu.ac.kr
Dae-Hyeong Kim, Center for Nanoparticle Research of the Institute for Basic Science, and School of Chemical and Biological Engineering, Seoul National University, South Korea; dkim98@snu.ac.kr
RicardoRuiz,LawrenceBerkeleyNationalLaborator y, USA; Ricardo.Ruiz@lbl.gov
Maryann C. Tung, Stanford University, USA; tungmc@stanford.edu
H.S. Philip Wong, Department of Engineering, Stanford University, USA; hspwong@stanford.edu

But with the recent introduction of extreme ultraviolet (EUV) lithography and the maturity of multiple patterning, current patterning challenges have moved from resolution to stochastics, defects, edge placement, overlay error, and cost. Here, we review applications of DSA in microelectronics, noting that the shifting landscape will impact future DSA applications.

In one implementation of DSA, called chemoepitaxy,[3] sparse chemical guides with affinity to one of the two blocks are spaced at a pitch multiple of the BCP domain periodicity (L_0). The chemical guides anchor the BCP domains perpendicularly to the substrate and align them linearly or hexagonally for lamellar[4] and cylindrical BCPs,[5,6] respectively (**Figure 1**a top-left and bottom-left). The large-scale periodicity of these chemoepitaxy films make them ideal for bit-patterned media (BPM).

For applications requiring aperiodic patterning, graphoepitaxy is more suitable[7,8] (Figure 1a top-right and bottom-right). In this process, topographical guides isolate small clusters of cylinders or lamellae, breaking the natural periodicity of the BCP. The number of domains in the cluster is flexible according to the chemical affinity and lateral dimensions of the guide. The ability to selectively place BCP domains has been critical to making BCP lithography compatible with the aperiodic layouts of ICs. Applications of graphoepitaxy include patterning contacts and vias for logic and memory devices,[9] as well as fins for FinFETs (Figure 1c).[10]

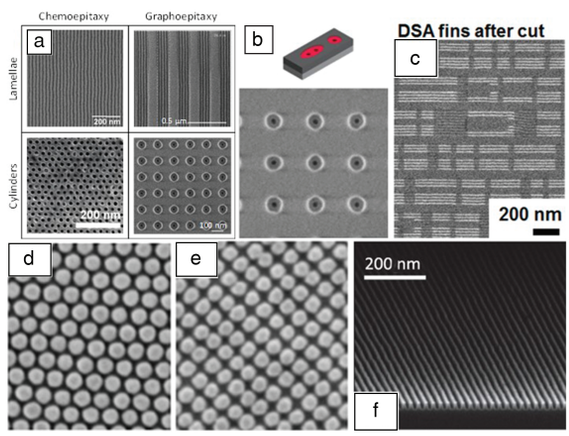

Figure 1. (a) Scanning electron microscope images for chemo- and graphoepitaxy with cylinder- and lamellae-forming block copolymers. Adapted with permission from Reference 4. © 2008 Wiley. Adapted with permission from Reference 7. © 2016 SPIE. Adapted with permission from Reference 6. © 2009 American Chemical Society. Adapted with permission from Reference 8. © 2015 American Vacuum Society. (b) Directed self-assembly (DSA) with cylindrical BCP ($L_0 = 30$ nm) in extreme ultraviolet -patterned guides. Adapted with permission from Reference 11. © 2016 SPIE. (c) Fins patterned by DSA for FinFET logic circuits. Adapted with permission from Reference 10. © 2014 American Chemical Society. (d, e) Finished magnetic bit patterned media at 1.2 and 1.6 Tdot/in^2 fabricated by block copolymer and nanoimprint lithography (d) in a 27.3-nm pitch hexagonal array, and (e) in a rectangular cell of 18.5 nm × 22 nm full pitch. Adapted with permission from Reference 19. © 2015 IEEE Magnetics Society. (f) Lamellae with 21.3-nm pitch produced by poly(2-vinyl pyridine)-*b*-polystyrene-*b*-poly(2-vinyl pyridine), a high-χ BCP, and transferred into Si. Adapted with permission from Reference 23. © 2016 IOP Publishing.

One use case of DSA is for the reduction of multiple-patterning steps in 193i and EUV through density multiplication. While BCPs are attractive for accessing sublithographic resolutions, implementation has been hampered by self-assembly defects. For cylindrical BCPs, high variability in the critical dimension (CD) of the domains and their placement has ruled out guides containing more than two to three cylinders and any nonlinear cylinder packing.[11] Similarly, the line roughness (LER) of lamellar domains deteriorates as the number of lamellae in the guide increases. These types of restrictions have diminished the viable density multiplication with DSA and lowered the potential reduction in patterning steps. Even so, DSA may still be a powerful method to extend the resolution of 193i and EUV, especially with DSA-aware design.[12]

In addition to density multiplication, DSA also has been shown to heal imperfect prepatterns, including LER and CD uniformity.[13] This feature rectification property is especially attractive for assisting EUV lithography, where sensitivity, roughness, and resolution are mutually exclusive.[14] Recent work has proposed using DSA as a complement to EUV to heal poor LER and resolution in EUV prepatterns.[15] This would allow chipmakers to use more sensitive EUV resists, or lower doses, thereby raising the throughput, and without sacrificing roughness and resolution.

Looking ahead to the 3-nm node and beyond, it is anticipated that sub-10 nm features will be required. However, BCPs with short L_0 can suffer from low segregation strength, self-assembling into morphologies with poor roughness, alignment, and other defects. Segregation strength is measured by χN, where χ is the Flory–Huggins parameter and N is the overall degree of polymerization. PS-b–PMMA, due to its relatively low χ, can only achieve reasonable segregation strength at $L_0 > 22$ nm.[16] For this reason, new higher-χ BCP chemistries are required for sub-10 nm patterning. These new chemistries show promise, enabling domains as small as 3 nm, but they have not reached maturity.[17]

While the current lithography ecosystem differs significantly from when BCP lithography was first introduced in the roadmap, DSA research has evolved to solve some of today's challenges in roughness, uniformity, edge placement error, and cost, by exploiting its small feature sizes, high feature uniformity, and self-repair property. Additionally, emerging applications of BCPs make use of the built-in chemical contrast of BCPs for novel etching and deposition processes, such as selective-area growth, selective-area etching, and sequential infiltration synthesis.[18] As the dimensions of ICs continue to shrink, the ability of BCPs to scale to sub-10 nm resolutions or even in three dimensions will only become more valuable.

For magnetic recording devices

The most aggressive quest for the smallest features in DSA lithography comes from the magnetic recording industry. In

magnetic BPM[19] the path to stable, denser media consists of replacing the clusters of randomly grouped grains in conventional media with lithographically defined magnetic islands (Figure 1d–e). For BPM to reach areal densities >2 Tdot/in^2, the critical dimensions need to be in the single-digit nanometer range. The unique geometrical design and the stringent requirements for BPM exemplify the extraordinary flexibility and value that DSA can bring to patterning applications. Beyond the sublithographic dimensions, BPM calls for dense, stitch-free patterns on circular tracks at constant angular pitch.

The pursuit of these goals has led to innovations in self-assembly and nanofabrication. A key breakthrough to reach sublithographic patterning came with feature density multiplication enabled by DSA from sparse patterning.[5] The flexibility of the BCP chains accommodates the slight distortions needed to direct the patterns onto circular tracks with constant angular pitch. The synergies between nanoimprint and BCP lithography[20] also enable a fast path to generate guiding patterns and a way to realize rectangular features from the striped lamellae-forming BCPs.[21] The push for small dimensions resulted in demonstrations of self-aligned double patterning from the BCP films[22] in combination with ALD infiltration[19] to increase feature densities by another factor of two. Significant progress in higher-χ BCP has led to pattern transfer demonstrations from 11 nm[23] (Figure 1f) down to 5 nm.[24] Finally, innovation in surface functionalization[25] and interfacial energy engineering[26] lead to clever two- and three-tone,[27] as well as sidewall chemical patterning[28] that is likely to find applications in many other fields.

While critical feasibility milestones were demonstrated such as integration with aperiodic servo patterns[29] and magnetic recording demonstrations[19,30] at densities ranging from 1–2 Tdot/in^2 (Figure 1d–e), other challenges loomed large for BPM technology. Ultimately, the lithographic difficulties to fabricate skinnier, longer bit cells with higher aspect ratios[19] to boost drive performance, integration challenges, cost pressures, a shifting market landscape, and the advent of other technologies such as three-dimensional flash and heat-assisted magnetic recording[31] all contributed to deprioritization of BPM. Nonetheless, the many contributions from BPM to block copolymer lithography will permeate as bottom-up patterning continues to evolve to other applications.

Colloidal nanocrystals and their assembly

Colloidal NPs are fragments of inorganic solids, having at least one dimension that is <100 nm in scale, with organic or inorganic ligands at their surfaces that enable their electrostatic or steric stabilization as dispersions in solvents. Gas-phase and wet-chemical synthetic techniques have been advanced to prepare colloidal NPs with exquisite control of their size, typically ranging from 2 to 100 nm; shape, such as spheres, rods, cubes, platelets, wires, and sheets; composition, including amorphous or crystalline elemental, binary, ternary, and quaternary compounds and alloys; and internal structure, in particular to form core–shell or Janus heterostructures.[32] This library of NPs includes metals, semiconductors, insulators, magnets, luminophores, and phase-change materials, among others and are often prized for their size-dependent physical properties such as tailorable localized surface plasmon resonances, absorption and luminescence, and superparamagnetism.

The library of established NP surface chemistries is also considerable, and includes inorganic ions, organic small- and biomolecules, and polymers.[33] These ligands allow the dispersion of NPs in solvents; their solution-based assembly via coating, casting, and printing techniques to form NP supercrystals and thin-film solids; and serve as "molecular rulers" to mediate the physical property interactions between NPs. The ligands may also add recognition, redox, and light absorption functions.

NP assemblies can adopt amorphous or crystalline architectures like those, and yet with observations of additional packing motifs, as atomic solids.[34] The organization depends on the balance of van der Waals, electrostatic, and/or magnetic interactions between the NPs, that are mediated by the ligand chemistry and solvent selection; and the time scale of solvent evaporation and freedom for NPs to reorganize on a solid or liquid surface, with methods of slow evaporation and deposition on liquid subphases favoring more ordered structures. Assemblies can be composed of a "mix and match" of NPs from the now vast library of building blocks to allow combinations of functions, even those that are "orthogonal" and typically not found in atomic solids. Solution-based assembly allows the low-cost, large-area integration of NPs and their solids in devices, which we describe here by their use in patterning conventional, and in constructing unconventional, electronic devices, including transistors and circuits, memory devices, light-emitting diodes (LEDs), biosensors, and electrical stimulators.[35,36]

For lithography and templating

The exquisite control over NP composition and uniformity make large-area superlattice assemblies also attractive for lithographic patterning, especially at <10 nm where traditional methods are prohibitively expensive or simply not accessible. Challenges include ligand removal,[37] high-contrast pattern transfer,[38] achieving uniform deposition of (sub-)monolayer NP assemblies over wafer scale, DSA[39] for orientation control, and feature registration and integration.[31]

Control over the self-assembly of colloidal NCs is highly intertwined with the type of capping ligand used.[34] The ligands used in synthesis leave an interparticle spacing too small for lithographic applications. Polymer-grafted NPs,[40] with a dense polymeric ligand shell (concentrated polymer brush regime) completely screen core–core interactions and provide a rich phase diagram in concentrated dispersions.[41,42] They are compatible with flow coating,[43] spin coating,[44] and dip coating[45] for large-area uniform deposition. The opportunity to vary chain length and grafting density opens several possibilities for rich structural diversity in particle blends.[46] Furthermore, solvent annealing may impart mobility to the polymer chains enabling

a thermodynamically driven self-assembly process toward equilibrium as opposed to the most commonly employed, kinetically driven, evaporation-controlled methods. This is a powerful method to achieve not only wafer-scale monolayer assemblies, but also integration with top-down templates for DSA.[44] The ability to tune the interparticle space by the polymer chain length opens the process window for pattern transfer. An additional layer of information content can be added if the polymeric ligand is a block copolymer chain.[47]

Functional building blocks for electronics

Colloidal metallic, semiconducting, and insulating NPs are used as the building blocks of device layers in unconventional electronic and optoelectronic devices. Ligands at the NP surfaces mediate charge transport and thus are often modified for use in devices. To create high conductivity metallic and high mobility semiconducting NP layers, the ligands introduced in synthesis, which often establish a ~2 nm interparticle distance, are exchanged for more compact moieties or stripped to decrease the distance and increase electronic coupling between NPs. For example, metal NP assemblies traverse an insulator-to-metal transition, seen by a 10^{10} change in conductivity, as ligand exchange reduces interparticle spacing from 2 nm to where the NPs touch and fuse.[48] Similarly, carrier mobility in semiconductor NP layers increases by ~10^5 upon ligand exchange and/or stripping.[49–51] In the case of semiconductor NP layers, surface modification with atoms, ions, or ligands are used in bandgap engineering of conduction- and valence-band states and to provide *n*- and *p*-doping. In contrast, insulating NPs may be supported by ligand selection to reduce device leakage and modify the dielectric constant of their layers.

As an example, ligand-engineered, metallic Ag, semiconducting CdSe, and insulating Al_2O_3 NPs were used as building blocks to realize the electrodes, channel, and gate dielectric layers, respectively, of all-NP solution-processable, low-voltage, high-mobility, field-effect transistors (**Figure 2**a–f).[52] Metallic In NPs are co-dispersed with Ag NPs to form the source and drain electrodes and provide a reservoir of indium, that upon annealing diffuses and thus passivates and *n*-dopes the CdSe NP channel layer. Integration of the different NP layers in the device stack requires the use of orthogonal solution-based processing and patterning methods—in this example photolithography is used—that do not alter the physical properties of the constituent NP layers. Interface engineering using surface modification methods are also used to ensure chemical compatibility, structural stability, and physical cooperation to realize high-performance NP devices. Figure 2g shows the gate-voltage modulated source-drain current-voltage characteristics for a representative all-NP, flexible, transistor.

High-mobility NP transistors, albeit where only the semiconducting channel was comprised of NPs and other device layers were fabricated using conventional techniques, have been used as building blocks to demonstrate integrated circuits (Figure 2h).[53] Vertical interconnect access holes are defined to construct circuit topologies and demonstrate NP amplifiers, ring oscillators, and NAND and NOR logic gates. These NP semiconductor channels form solution-processable ring oscillators with fast switching speeds at low voltages establishing NPs as a competitive materials class for large-area, flexible, high-speed circuits.

In these examples, long-studied CdSe NPs were used. Cd- and Pb-free NP compositions are similarly being developed to construct electronic devices and circuits.[54,55] Also in these examples, the chemical and thermal processes were selected to be compatible with device fabrication on flexible plastics,[56] as needed for wearable and implantable devices.

Wearable and implantable electronics

NP assemblies offer new physical, mechanical, and biomedical performance characteristics that cannot be achieved in devices based on conventional bulk materials.[57] One notable feature of such devices is their soft mechanical nature.[58] The nanoscale dimension of the materials dramatically reduces their flexural rigidity.[59] The resultant devices can be seamlessly integrated with soft curvilinear human bodies to monitor biosignals, to store the recorded data, to display the processed data, and to apply feedback stimulations. Example devices include

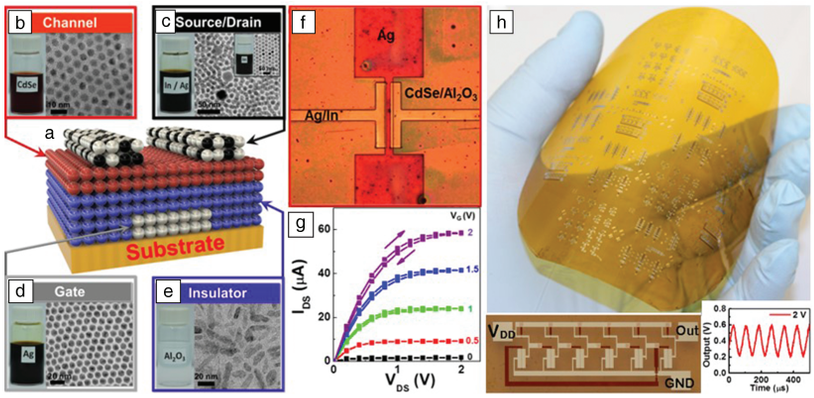

Figure 2. (a) Solution-processable, field-effect transistor assembled from colloidal nanoparticles (NPs) of (b) semiconducting CdSe, to form the channel, (c) metallic Ag and In, to create the source and drain electrodes, (d) metallic Ag, to define the gate, and (e) insulating Al_2O_3 NPs to form the gate dielectric layer. (f) All-NP transistor fabricated on flexible Kapton and its (g) output characteristics of drain–current I_D versus source–drain voltage, V_{DS}, as a function of the applied gate voltage, V_G. (h) Photograph of CdSe NP integrated circuits fabricated across a 4″ diameter flexible Kapton substrate, and inset, a photograph and output characteristics of a five-stage ring oscillator with a sixth-stage buffer. (a–g) Reprinted with permission from Reference 52. © 2016 AAAS. (h) Adapted with permission from Reference 53. © 2015 American Chemical Society.

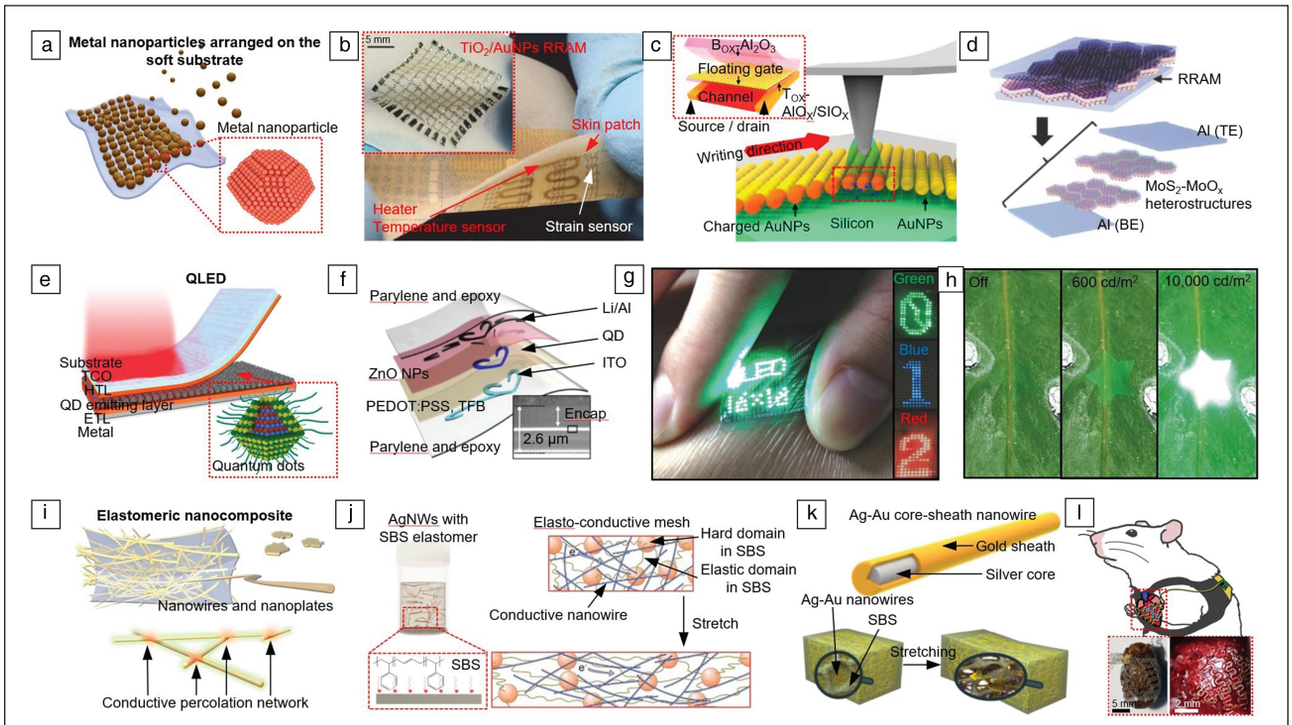

Figure 3. (a) Nanoparticle (NP) monolayer assembled on a flexible substrate. (b) Photograph of a wearable system comprised of a strain gauge, (inset) a TiO_2/Au NP resistive random access memory (RRAM), and a thermal actuator. (c) Schematic of charge injection into Au NPs in a flash memory. Schematic of (d) a RRAM based on a MoS_2-MoO_x heterostructure, and of (e) a quantum dot light-emitting diode (QDLED) and (f) wearable QDLED. Inset, a cross-sectional scanning electron microscope image of the QDLED. (g) Photograph of a wearable passive matrix QDLED on skin, (inset) green, blue, and red QDLEDs. Reprinted with permission from Reference 64. © 2017 Wiley. (h) Transparent QDLEDs on a leaf. Reprinted with permission from Reference 65. © 2018 Wiley. (i) Schematic of a stretchable conductive nanocomposite (top), and a percolation network inside the nanocomposite (bottom). (j) Schematic of nanowires in an elastomer. Reprinted with permission from Reference 67. © 2016 AAAS. (k) Schematic of an Ag-Au core-sheath nanowire (top) and the nanocomposite before and after stretching (bottom). (1) Schematic and photograph of an epicardial mesh. Reprinted with permission from Reference 69. © 2020 Wiley.

wearable electronic devices, quantum-dot-based wearable LEDs, and nanowire-composite-based wearable and implantable devices.

The assembly of metal NPs, as a monolayer or a few layers, and their integration inside electronics brings distinctive enhancement in device performance (**Figure 3**a). For example, Figure 3b shows a wearable biosensing and data storage device, which consists of an array of strain sensors and resistive random-access memory (RRAM).[60] The ultrathin and stretchable nature of the device enables its conformal integration on the human skin. Therefore, the strain sensor based on Si nanomembranes can measure muscular tremors precisely without motion artefacts, and the recorded signals can be stored in the RRAM array. Note that Au NPs are assembled by the Langmuir–Blodgett assembly method inside TiO_2 nanomembranes of the RRAM, and thereby the performance of the memory device can be dramatically increased. These wearable devices are considered as a promising solution to acquire, store, and process a large set of biomedical data toward next-generation digital healthcare. The device performance can be improved further by utilizing other combinations of nanomaterials and devices, such as Au NPs on Si nanomembranes for the charge trap floating gate memory (Figure 3c)[61] or molybdenum disulfide (MoS_2) nanosheets with molybdenum oxide nanomembranes for the RRAM (Figure 3d).[62]

Another important type of nanomaterial-based electronics is wearable quantum dot light-emitting diodes (QDLEDs) (Figure 3e). Among various light-emitting devices, ultrathin QDLEDs are highlighted due to their unique characteristics, including high brightness, color purity, superb printability, and soft form factors. A high-resolution form of wearable QDLEDs was developed by using the intaglio transfer-printing technique (Figure 3f).[63] In this process, a stamp fully-inked with QDs is contacted on an intaglio trench in a silicon wafer, the stamp with QDs is detached from the silicon wafer, and the remaining QDs on the stamp are transfer-printed to a receiver substrate. This novel QD patterning method enables full-color QD arrays with a resolution of 2460 pixels per inch. The ultrathin QDLEDs can be laminated on various curvilinear surfaces, including the human skin, and display the recorded signals from the sensors in real-time when integrated with wearable biosensors. For example, the wearable system can monitor temperature changes and body motions, and visualize them on the subject's skin (Figure 3g).[64] Further improvements in terms of user friendliness can be achieved by developing a transparent form of the wearable QDLEDs. The transparent wearable

QDLEDs feature an extremely high luminance (~73,000 cd m^{-2} at 9 V) and transmittance (90% at 550 nm, 84% over visible range), achieving invisibility on the human skin, which provides aesthetic advantages (Figure 3h).[65]

Meanwhile, stretchable conductive nanocomposites have been considered as a feasible alternative to conventional rigid metal electrodes in soft electronics (Figure 3i). Nanoscale metallic materials form a percolation network inside an elastomeric media, offering high conductivity and stretchability. The soft mechanical nature of the nanocomposite minimizes side effects from long-term biointegration of the devices, while the high conductivity maximizes the efficiency of the electrophysiological recording and feedback stimulation.

Previous approaches for the nanocomposites were typically to mix Ag nanowires with a rubber (Figure 3j).[66,67] But this method has shown limitations in terms of biocompatibility, oxidation resistance, conductivity, and stretchability. Recently, a nanocomposite based on ultralong core–shell nanowires with an Ag core and an Au shell was developed (Figure 3k).[68] The high aspect ratio of the core Ag nanowire conferred high conductivity in the nanocomposite, while the inert Au sheath achieved both biocompatibility and oxidation resistance. Phase separation inside the elastomeric block-*co*-polymer matrix induces microscale assembly of nanowires and improves both stretchability and conductivity. The nanocomposite was applied to soft bioelectronics, which recorded electrocardiography (ECG) signals and applied stimulations for feedback modulations. The addition of Pt microparticles enhances the performance further by decreasing the impedance (Figure 3l).[69]

NP-based soft electronics dramatically improve device performance as well as provide novel device functions. Despite such progress, numerous issues still remain toward the commercialization of the NP-based electronics, with regard to the long-term reliability of the materials and devices, the biocompatibilty *in vivo* for human-friendly applications, and the integration with other device units to build standalone systems. NPs and their assemblies, those with organic surface ligands in particular, morph inside the device under electron and hole flows, which can cause the migration of material and the formation of electrical defects. Although most materials are stable in their bulk state, new biological, chemical, and physical instabilities, including toxicity issues, arise in their nanoscale dimension. Novel NP synthesis methods and device design approaches are thereby required to secure long-term biocompatibility.[70,71] To build an integrated system including standalone type personalized wearable mobile electronics, the NP-based electronic devices should be connected with other device units, including power supply and wireless communication modules,[72,73] which often requires modification of material compositions and device designs of the NP-based electronics. Despite these remaining issues, the potential of the NP-based soft bioelectronics is so great that overarching clinical challenges are expected to be solved while many novel industrial opportunities are to be created.

Biomolecules (semiconductor synthetic biology)

For decades, progress in semiconductor technology was fueled by the scalability of lithographic patterning, enabling a continuous growth of faster, smaller, and less expensive transistors. Today, with escalating fabrication costs and increasing challenges to reach dimensions <10 nm, it is clear that the future of semiconductor scaling is shifting, presenting opportunities for disruption. The nascent field of semiconductor synthetic biology (SemiSynBio) is exploring pathways to exploit the advantages of biomolecular systems to advance semiconductor technology.[74] In this context, self-assembly of sequence-defined, synthetic biomolecules, including DNA, RNA, polypeptoids, and proteins may provide the necessary breakthroughs to next-generation nanomanufacturing for microelectronics. Some notable examples include directed assembly of DNA origami,[75] biotin-labelled DNA nanogrids,[76] directed assembly of fibrinogen proteins on PS-b-PMMA block copolymers[77] and NP superlattices via template-confined DNA-mediated assembly[78] (**Figure 4**a–d**)**. While this field is still in its infancy and several challenges need to be addressed in terms of stability, throughput, error rates, and compatibility, biomolecular assemblies may provide the solutions needed in terms of dimensions, information content, functionality, and modularity to extend semiconductor device fabrication.

Summary and outlook

Self-assembly of molecules, polymers, and NPs is enabling exquisite control of materials structure and function that arises

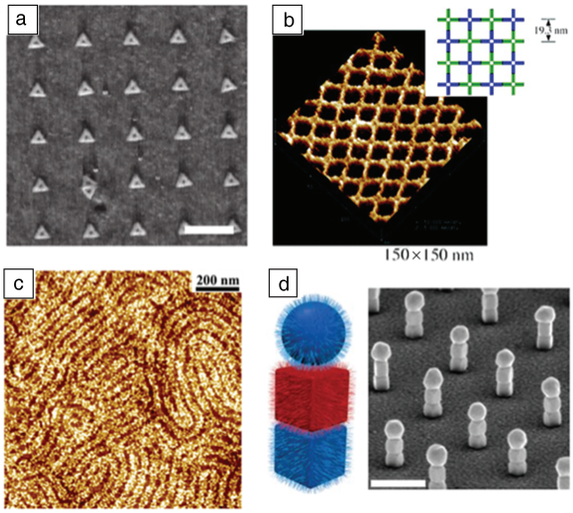

Figure 4. (a) Directed assembly of DNA origami. Adapted with permission from Reference 75. © 2014 American Chemical Society. (b) Biotin-labelled nanogrids. Reprinted with permission from Reference 76. © 2003 AAAS. (c) Fibrinogen proteins directed assembly on PS-*b*-PMMA block copolymer film. Adapted with permission from Reference 77. © 2016 American Chemical Society. (d) Cube-cube-sphere nanoparticle superlattices via template-confined DNA-mediated assembly. Adapted with permission from Reference 78. © 2018 AAAS.

for length scales at and below the ~10 nm scale. Even as the challenges in state-of-the-art lithography evolve, BCPs and biomolecules continue to be an attractive solution for patterning semiconductor and magnetic recording devices. DSA promises not only high resolution and good feature uniformity, but also self-repair and unique chemical contrast that can act as a powerful complement to optical and EUV lithography. Colloidal NP assemblies open up the synthesis of materials with "designer," single and multiple properties, not typically found in bulk materials, that exploit the size-dependent properties of and coupling of many similar and dissimilar NPs. As colloids, NPs allow for (hetero-)integration of materials with conventional and increasingly unconventional devices to meet the growing demand for flexible, wearable, and implantable electronics.

Acknowledgments

C.R.K. is grateful for support from the National Science Foundation (NSF) Materials Research Science and Engineering Center (MRSEC) under Award No. DMR-1720530. T.H. and D.-H.K. acknowledge support from the Institute for Basic Science (IBS-R006-A1 and IBS-R006-D1). M.C.T. is supported in part by an NSF Graduate Research Fellowship. H.S.P.W. acknowledges support from the Stanford Non-Volatile Memory Technology Initiative and the Stanford SystemX Alliance. Work at the Molecular Foundry was supported by the Office of Science, Office of Basic Energy Sciences, of the U.S. Department of Energy under Contract No. DE-AC02-05CH11231.

References

1. F.S. Bates, G.H. Fredrickson, *Phys. Today* **52**, 32 (1999).
2. J.G. Son, K.W. Gotrik, C.A. Ross, *ACS Macro Lett.* **1**, 1279 (2012).
3. C.-C. Liu, E. Han, M.S. Onses, C.J. Thode, S. Ji, P. Gopalan, P.F. Nealey, *Macromolecules* **44**, 1876 (2011).
4. J.Y. Cheng, C.T. Rettner, D.P. Sanders, H.-C. Kim, W.D. Hinsberg, *Adv. Mater.* **20**, 3155 (2008).
5. R. Ruiz, H. Kang, F.A. Detcheverry, E. Dobisz, D.S. Kercher, T.R. Albrecht, J.J. de Pablo, P.F. Nealey, *Science (80).* **321**, 936 (2008).
6. L. Wan, X. Yang, *Langmuir* **25**, 12408 (2009).
7. G. Claveau, P. Quemere, M. Argoud, J. Hazart, P.P. Barros, A. Sarrazin, N. Posseme, R. Tiron, X. Chevalier, C. Nicolet, C. Navarro, *J. Micro-Nanolith. MEM.* **15**, 031604 (2016).
8. J. Doise, J. Bekaert, B.T. Chan, R. Gronheid, Y. Cao, S. Hong, G. Lin, D. Fishman, Y. Chakk, T. Marzook, *J. Vac. Sci. Technol. B.* **33**, 06F301 (2015).
9. X.-Y. Bao, H. Yi, C. Bencher, L.-W. Chang, H. Dai, Y. Chen, P.-T.J. Chen, H.-S.P. Wong, *2011 International Electron Devices Meeting* (IEEE, Washington, DC, 2011), http://ieeexplore.ieee.org/document/6131510/), pp. 7.7.1–7.7.4.
10. H. Tsai, J.W. Pitera, H. Miyazoe, S. Bangsaruntip, S.U. Engelmann, C.-C. Liu, J.Y. Cheng, J.J. Bucchignano, D.P. Klaus, E.A. Joseph, D.P. Sanders, M.E. Colburn, M.A. Guillorn, *ACS Nano* **8**, 5227 (2014).
11. I. Karageorgos, J. Ryckaert, M.C. Tung, H.-S.P. Wong, R. Gronheid, J. Bekaert, E. Karageorgos, K. Croes, G. Vandenberghe, M. Stucchi, W. Dehaene, L. Capodieci, J.P. Cain, Eds. (International Society for Optics and Photonics, San Jose, CA, 2016), http://proceedings.spiedigitallibrary.org/proceeding.aspx?doi=10.1117/12.2222041), vol. 9781, p. 97810N.
12. H. Yi, X.-Y. Bao, R. Tiberio, H.-S.P. Wong, *Nano Lett.* **15**, 805 (2015).
13. S.-J. Jeong, J.Y. Kim, B.H. Kim, H.-S. Moon, S.O. Kim, *Mater. Today* **16**, 468 (2013).
14. T.A. Brunner, X. Chen, A. Gabor, C. Higgins, L. Sun, C.A. Mack, E.M. Panning, K.A. Goldberg, Eds. (International Society for Optics and Photonics, San Jose, CA, 2017), http://proceedings.spiedigitallibrary.org/proceeding.aspx?doi=10.1117/12.2258660), vol. 10143, p. 101430E.
15. R. Gronheid, C. Boeckx, J. Doise, J. Bekaert, I. Karageorgos, J. Ruckaert, B.T. Chan, C. Lin, Y. Zou, E.M. Panning, K.A. Goldberg, Eds. (International Society for Optics and Photonics, San Jose, CA, 2016), http://proceedings.spiedigitallibrary.org/proceeding.aspx?doi=10.1117/12.2219876), vol. 9776, p. 97761W.
16. L. Wan, R. Ruiz, H. Gao, K.C. Patel, T.R. Albrecht, J. Yin, J. Kim, Y. Cao, G. Lin, *ACS Nano* **9**, 7506 (2015).
17. C.M. Bates, M.J. Maher, D.W. Janes, C.J. Ellison, C.G. Willson, *Macromolecules* **47**, 2 (2014).
18. Q. Peng, Y.-C. Tseng, S.B. Darling, J.W. Elam, *ACS Nano* **5** (6), 4600 (2011).
19. T.R. Albrecht, H. Arora, V. Ayanoor-Vitikkate, J.-M. Beaujour, D. Bedau, D. Berman, A.L. Bogdanov, Y.-A. Chapuis, J. Cushen, E.E. Dobisz, G. Doerk, H. Gao, M. Grobis, B. Gurney, W. Hanson, O. Hellwig, T. Hirano, P.-O. Jubert, D. Kercher, J. Lille, Z. Liu, C.M. Mate, Y. Obukhov, K.C. Patel, K. Rubin, R. Ruiz, M. Schabes, Wan, D. Weller, T.-W. Wu, E. Yang, *IEEE Trans. Magn.* **51**, 1 (2015).
20. X. Yang, S. Xiao, W. Hu, J. Hwu, R. van de Veerdonk, K. Wago, K. Lee, D. Kuo, *Nanotechnology* **25**, 395301 (2014).
21. L. Wan, R. Ruiz, H.H. Gao, K.C. Patel, J. Lille, G. Zeltzer, E.A. Dobisz, A. Bogdanov, T.R. Albrecht, P.F. Nealey, *J. Micro/Nanolithography MEMS MOEMS* **11** (3), 031405 (2012).
22. G.S. Doerk, H. Gao, L. Wan, J. Lille, K.C. Patel, Y.-A. Chapuis, R. Ruiz, T.R. Albrecht, *Nanotechnology* **26**, 085304 (2015).
23. S. Xiong, Y.-A. Chapuis, L. Wan, H. Gao, X. Li, R. Ruiz, P.F. Nealey, *Nanotechnology* **27**, 415601 (2016).
24. A.P. Lane, X. Yang, M.J. Maher, G. Blachut, Y. Asano, Y. Someya, A. Mallavarapu, S.M. Sirard, C.J. Ellison, C.G. Willson, *ACS Nano* **11**, 7656 (2017).
25. L. Wan, R. Ruiz, *ACS Appl. Mater. Interface.* **11**, 20333 (2019).
26. C.M. Bates, T. Seshimo, M.J. Maher, W.J. Durand, J.D. Cushen, L.M. Dean, G. Blachut, C.J. Ellison, C.G. Willson, *Science (80).* **338**, 775 (2012).
27. L.D. Williamson, R.N. Seidel, X. Chen, H.S. Suh, P. Rincon Delgadillo, R. Gronheid, P.F. Nealey, *ACS Appl. Mater. Interfaces* **8**, 2704 (2016).
28. J. Cushen, L. Wan, G. Blachut, M.J. Maher, T.R. Albrecht, C.J. Ellison, C.G. Willson, R. Ruiz, *ACS Appl. Mater. Interfaces* **7**, 13476 (2015).
29. S. Xiao, X. Yang, P. Steiner, Y. Hsu, K. Lee, K. Wago, D. Kuo, *ACS Nano* **8**, 11854 (2014).
30. X. Yang, S. Xiao, Y. Hsu, H. Wang, J. Hwu, P. Steiner, K. Wago, K. Lee, D. Kuo, *J. Micro-Nanolith. MEM.* **13**, 031307 (2014).
31. K. Hono, Y.K. Takahashi, G. Ju, J.-U. Thiele, A. Ajan, X. Yang, R. Ruiz, L. Wan, *MRS Bull.* **43**, 93 (2018).
32. P. Reiss, M. Carrière, C. Lincheneau, L. Vaure, S. Tamang, *Chem. Rev.* **116**, 10731 (2016).
33. M.A. Boles, D. Ling, T. Hyeon, D.V. Talapin, *Nat. Mater.* **15**, 141 (2016).
34. M.A. Boles, M. Engel, D.V. Talapin, *Chem. Rev.* **116**, 11220 (2016).
35. C.R. Kagan, E. Lifshitz, E.H. Sargent, D.V. Talapin, *Science (80)*, **353**, aac5523 (2016).
36. J. Yang, M.K. Choi, D.-H. Kim, T. Hyeon, *Adv. Mater.* **28**, 1176 (2016).
37. S. Shaw, T.F. Silva, J.M. Bobbitt, F. Naab, C.L. Rodrigues, B. Yuan, J.J. Chang, X. Tian, E.A. Smith, L. Cademartiri, *Chem. Mater.* **29**, 7888 (2017).
38. C. Hogg, Y. Picard, A. Narasimhan, J. Bain, S. Majetich, *Nanotechnology* **24** (2013), doi:10.1088/0957–4484/24/8/085303.
39. M. Asbahi, S. Mehraeen, F. Wang, N. Yakovlev, K.S.L. Chong, J. Cao, M.C. Tan, J.K.W. Yang, *Nano Lett.* **15**, 6066 (2015).
40. C. Yi, Y. Yang, B. Liu, J. He, Z. Nie, *Chem. Soc. Rev.* **49**, 465 (2020).
41. C.N. Likos, *Soft Matter* **2**, 478 (2006).
42. H. Yun, J.W. Yu, Y.J. Lee, J.-S. Kim, C.H. Park, C. Nam, J. Han, T.-Y. Heo, S.-H. Choi, D.C. Lee, W.B. Lee, G.E. Stein, B.J. Kim, *Chem. Mater.* **31**, 5264 (2019).
43. J. Che, K. Park, C.A. Grabowski, A. Jawaid, J. Kelley, H. Koerner, R.A. Vaia, *Macromolecules* **49**, 1834 (2016).
44. J. Chen, A. Fasoli, J.D. Cushen, L. Wan, R. Ruiz, *Macromolecules* **50**, 9636 (2017).
45. A. Watanabe, N. Kihara, T. Okino, R. Yamamoto, *J. Photopolym. Sci. Technol.* **28**, 643 (2015).
46. X. Ye, C. Zhu, P. Ercius, S.N. Raja, B. He, M.R. Jones, M.R. Hauwiller, Y. Liu, T. Xu, A.P. Alivisatos, *Nat. Commun.* **6**, 10052 (2015).
47. V.B. Leffler, L. Mayr, P. Paciok, H. Du, R.E. Dunin-Borkowski, M. Dulle, S. Förster, *Angew. Chem. Int. Ed.* **58**, 8541 (2019).
48. A.T. Fafarman, S.-H. Hong, H. Caglayan, X. Ye, B.T. Diroll, T. Paik, N. Engheta, C.B. Murray, C.R. Kagan, *Nano Lett.* **13**, 350 (2013).
49. C.R. Kagan, C.B. Murray, *Nat. Nanotechnol.* **10**, 1013 (2015).
50. J.-S. Lee, M. V Kovalenko, J. Huang, D.S. Chung, D.V Talapin, *Nat. Nanotechnol.* **6**, 348 (2011).
51. J.-H.H. Choi, A.T. Fafarman, S.J. Oh, D.-K.K. Ko, D.K. Kim, B.T. Diroll, S. Muramoto, G. Gillen, C.B. Murray, C.R. Kagan, J.G. Gillen, C.B. Murray, C.R. Kagan, *Nano Lett.* **12**, 2631 (2012).
52. J.-H. Choi, H. Wang, S.J. Oh, T. Paik, P.S. Jo, J. Sung, X. Ye, T. Zhao, B.T. Diroll, C.B. Murray, C.R. Kagan, *Science (80).* **352** (2016), doi:10.1126/science.aad0371.
53. F.S. Stinner, Y. Lai, D.B. Straus, B.T. Diroll, D.K. Kim, C.B. Murray, C.R. Kagan, *Nano Lett.* **15**, 7155 (2015).
54. W. Liu, J.-S. Lee, D.V Talapin, *J. Am. Chem. Soc.* **135**, 1349 (2013).
55. H. Wang, D.J. Butler, D.B. Straus, N. Oh, F. Wu, J. Guo, K. Xue, J.D. Lee, C.B. Murray, C.R. Kagan, *ACS Nano* **13**, 2324 (2019).
56. C.R. Kagan, *Chem. Soc. Rev.* **48**, 1626 (2019).
57. S. Choi, H. Lee, R. Ghaffari, T. Hyeon, D.-H. Kim, *Adv. Mater.* **28**, 4203 (2016).

58. J. Kim, R. Ghaffari, D.-H. Kim, *Nat. Biomed. Eng.* **1**, 0049 (2017).
59. J.A. Rogers, M.G. Lagally, R.G. Nuzzo, *Nature* **477**, 45 (2011).
60. D. Son, J. Lee, S. Qiao, R. Ghaffari, J. Kim, J.E. Lee, C. Song, S.J. Kim, D.J. Lee, S.W. Jun, S. Yang, M. Park, J. Shin, K. Do, M. Lee, K. Kang, C.S. Hwang, N. Lu, T. Hyeon, D.-H. Kim, *Nat. Nanotechnol.* **9**, 397 (2014).
61. J. Kim, D. Son, M. Lee, C. Song, J.-K. Song, J.H. Koo, D.J. Lee, H.J. Shim, J.H. Kim, M. Lee, T. Hyeon, D.-H. Kim, *Sci. Adv.* **2**, e1501101 (2016).
62. D. Son, S.I. Chae, M. Kim, M.K. Choi, J. Yang, K. Park, V.S. Kale, J.H. Koo, C. Choi, M. Lee, J.H. Kim, T. Hyeon, D.-H. Kim, *Adv. Mater.* **28**, 9326 (2016).
63. M.K. Choi, J. Yang, K. Kang, D.C. Kim, C. Choi, C. Park, S.J. Kim, S.I. Chae, T.-H. Kim, J.H. Kim, T. Hyeon, D.-H. Kim, *Nat. Commun.* **6**, 7149 (2015).
64. J. Kim, H.J. Shim, J. Yang, M.K. Choi, D.C. Kim, J. Kim, T. Hyeon, D.-H. Kim, *Adv. Mater.* **29**, 1700217 (2017).
65. M.K. Choi, J. Yang, D.C. Kim, Z. Dai, J. Kim, H. Seung, V.S. Kale, S.J. Sung, C.R. Park, N. Lu, T. Hyeon, D.-H. Kim, *Adv. Mater.* **30**, 1703279 (2018).
66. S. Choi, J. Park, W. Hyun, J. Kim, J. Kim, Y.B. Lee, C. Song, H.J. Hwang, J.H. Kim, T. Hyeon, D.-H. Kim, *ACS Nano* **9**, 6626 (2015).
67. J. Park, S. Choi, A.H. Janardhan, S.-Y. Lee, S. Raut, J. Soares, K. Shin, S. Yang, C. Lee, K.-W. Kang, H.R. Cho, S.J. Kim, P. Seo, W. Hyun, S. Jung, H.-J. Lee, N. Lee, S.H. Choi, M. Sacks, N. Lu, M.E. Josephson, T. Hyeon, D.-H. Kim, H.J. Hwang, *Sci. Transl. Med.* **8**, 344ra86 (2016).
68. S. Choi, S.I. Han, D. Jung, H.J. Hwang, C. Lim, S. Bae, O.K. Park, C.M. Tschabrunn, M. Lee, S.Y. Bae, J.W. Yu, J.H. Ryu, S.-W. Lee, K. Park, P.M. Kang, W.B. Lee, R. Nezafat, T. Hyeon, D.-H. Kim, *Nat. Nanotechnol.* **13**, 1048 (2018).
69. S. Sunwoo, S.I. Han, H. Kang, Y.S. Cho, D. Jung, C. Lim, C. Lim, M. Cha, S. Lee, T. Hyeon, D. Kim, *Adv. Mater. Technol.* **5**, 2070014 (2020).
70. C. Choi, M.K. Choi, S. Liu, M.S. Kim, O.K. Park, C. Im, J. Kim, X. Qin, G.J. Lee, K.W. Cho, M. Kim, E. Joh, J. Lee, D. Son, S.-H. Kwon, N.L. Jeon, Y.M. Song, N. Lu, D.-H. Kim, *Nat. Commun.* **8**, 1664 (2017).
71. J. Lee, H.R. Cho, G.D. Cha, H. Seo, S. Lee, C.-K. Park, J.W. Kim, S. Qiao, L. Wang, D. Kang, T. Kang, T. Ichikawa, J. Kim, H. Lee, W. Lee, S. Kim, S.-T. Lee, N. Lu, T. Hyeon, S.H. Choi, D.-H. Kim, *Nat. Commun.* **10**, 5205 (2019).
72. H. Lee, T.K. Choi, Y.B. Lee, H.R. Cho, R. Ghaffari, L. Wang, H.J. Choi, T.D. Chung, N. Lu, T. Hyeon, S.H. Choi, D.-H. Kim, *Nat. Nanotechnol.* **11**, 566 (2016).
73. K.W. Cho, S.J. Kim, J. Kim, S.Y. Song, W.H. Lee, L. Wang, M. Soh, N. Lu, T. Hyeon, B.-S. Kim, D.-H. Kim, *Nat. Commun.* **10**, 4824 (2019).
74. M. Bathe, L.A. Chrisey, D.J.C. Herr, Q. Lin, D. Rasic, A.T. Woolley, R.M. Zadegan, V.V. Zhirnov, *Nano Futures* **3**, 012001 (2019).
75. A. Gopinath, P.W.K. Rothemund, *ACS Nano* **8**, 12030 (2014).
76. H. Yan, S.H. Park, G. Finkelstein, J.H. Reif, T.H. LaBean, *Science* (**80**), 301 (2003).
77. T. Xie, A. Vora, P.J. Mulcahey, S.E. Nanescu, M. Singh, D.S. Choi, J.K. Huang, C.C. Liu, D.P. Sanders, J.I. Hahm, *ACS Nano* **10**, 7705 (2016).
78. Q.Y. Lin, J.A. Mason, Z. Li, W. Zhou, M.N. O'Brien, K.A. Brown, M.R. Jones, S. Butun, B. Lee, V.P. Dravid, K. Aydin, C.A. Mirkin, *Science* (**80**), 359 (2018). □